DATA ONLY

PHYSICAL REVIEW B VOLUME 60, NUMBER 6 1 AUGUST 1999-II

Chemical bonding in Tl cuprates studied by x-ray photoemission

R. P. Vasquez*
Center for Space Microelectronics Technology, Jet Propulsion Laboratory, California Institute of Technology, Pasadena, California 91109-8099

M. P. Siegal and D. L. Overmyer
Sandia National Laboratories, Albuquerque, New Mexico 87185-1421

Z. F. Ren, J. Y. Lao, and J. H. Wang
Materials Synthesis Laboratory, Department of Chemistry, State University of New York, Buffalo, New York 14260-3000
(Received 9 March 1999)

Epitaxial thin films of the Tl cuprate superconductors $Tl_2Ba_2CaCu_2O_8$, $Tl_2Ba_2Ca_2Cu_3O_{10}$, and $Tl_{0.78}Bi_{0.22}Ba_{0.4}Sr_{1.6}Ca_2Cu_3O_{9-\delta}$ are studied with x-ray photoemission spectroscopy. These data, together with previous measurements in this lab of $Tl_2Ba_2CuO_{6+\delta}$ and $TlBa_2CaCu_2O_{7-\delta}$, comprise a comprehensive data set for a comparative study of Tl cuprates with a range of chemical and electronic properties. In the Cu $2p$ spectra, a larger energy separation between the satellite and main peaks (E_s-E_m) and a lower intensity ratio (I_s/I_m) are found to correlate with higher values of T_c. Analysis of these spectra within a simple configuration interaction model suggests that higher values of T_c are related to low values of the O $2p\rightarrow$Cu $3d$ charge transfer energy. In the O $1s$ region, a smaller bond length between Ba and Cu-O planar oxygen is found to correlate with a lower binding energy for the signal associated with Cu-O bonding, most likely resulting from the increased polarization screening by Ba^{2+} ions. For samples near optimum doping, maximum T_c is observed to occur when the Tl $4f_{7/2}$ binding energy is near 117.9 eV, which is near the middle of the range of values observed for Tl cuprates. Higher Tl $4f_{7/2}$ binding energies, corresponding to formal oxidation states nearer Tl^{1+}, are also found to correlate with longer bond lengths between Ba and Tl-O planar oxygen, and with higher binding energies of the O $1s$ signal associated with Tl-O bonding. [S0163-1829(99)12729-2]

I. INTRODUCTION

The Tl-based tetragonal cuprate superconductors of the form $Tl_mBa_2Ca_{n-1}Cu_nO_{2n+m+2\pm\delta}$ ($m=1,2$; $n=1,2,3$), commonly abbreviated Tl-$m2(n-1)n$, are a class of materials in which the chemical and electronic properties, for which photoemission is a sensitive probe, vary with the number of Tl-O and Cu-O layers. In tetragonal cuprate superconductors, a van Hove singularity (VHS) is typically located near or below the Fermi level (E_F),[1] thus requiring synthesis in an oxidizing atmosphere to optimize the hole doping and the superconducting transition temperature T_c, as in the double Tl-O layer materials. However, the stoichiometric ($\delta=0$) single Tl-O layer materials are hole overdoped and a VHS lies above E_F,[2] thus oxygen deficiency, sometimes requiring post-synthesis annealing in a reducing atmosphere,[3–5] or partial substitution of trivalent rare earth ions on the Ca site[6] is necessary for optimum T_c. The variation of E_F with oxygen stoichiometry is detectable in rigid shifts of the photoemission core levels, as previously reported for Tl-2201 (Ref. 7) and Tl-1212 (Ref. 2).

The Cu-O bonding varies with the number of Cu-O layers, with the oxygen coordination being distorted octahedral[8] for $n=1$, square pyramidal[9,10] for $n=2$, and a mixture of square pyramidal (outer Cu-O layers) and square planar (middle Cu-O layer) (Refs. 10–12) for $n=3$. It has been proposed that such differences in Cu-O bonding result in differences in Cu-apical oxygen charge transfer which are detectable in the Cu $2p$ photoemission spectra.[13] The Cu $2p$ spectra have also been analyzed within a simple configuration interaction model utilizing a two-band Hamiltonian.[14–17] Within this model, the O $2p\rightarrow$Cu $3d$ charge transfer energy Δ, the O $2p$-Cu $3d$ hybridization strength T, and the on-site Coulomb interaction between Cu $2p$ and Cu $3d$ holes U, are related to the experimentally determined energy separation between the poorly screened satellite and well-screened main peak (E_s-E_m) and to the ratio of the intensities of the satellite and main peak (I_s/I_m). Attempts to determine systematic trends in the Cu-O bonding parameters for the superconducting cuprates have yielded contradictory results, with some studies reporting that I_s/I_m (and Δ/T) increases with increasing T_c (e.g., Refs. 18 and 19) and other studies reporting the opposite (e.g., Refs. 20 and 21). These contradictory results may be related to differences in doping (oxygen content) between the samples studied by different groups, at least in the surface region probed by photoemission, since I_s/I_m depends sensitively on doping.[16,18–20] Surface preparation which avoids loss of oxygen is thus critical in such studies.

The Tl-O bonding also varies with the number of Tl-O layers, with Tl being bonded to (in addition to the long planar Tl-O bonds) two apical oxygens[9,11,12] for $m=1$, and to one apical oxygen and one oxygen in the adjacent Tl-O layer[9,10] for $m=2$. It has been reported that the single and double Tl-O layer materials have distinguishable photoemission spectra which reflect differences in charge transfer between Tl-O and Cu-O layers.[22]

In this work, x-ray photoemission spectroscopy (XPS)

measurements of Tl-2212, Tl-2223, and the Tl-1223 phase $Tl_{0.78}Bi_{0.22}Ba_{0.4}Sr_{1.6}Ca_2Cu_3O_{9-\delta}$ [(Tl, Bi)-1223] are reported which, together with previously reported measurements in this lab of Tl-2201 (Ref. 7) and Tl-1212 (Ref. 2), comprise a comprehensive comparative study of Tl cuprates with a range of chemical and electronic properties. These results are compared to earlier studies which have included comparison of several Tl cuprates,[20–23] as well as studies of individual Tl cuprate phases.[20,24–26]

II. EXPERIMENTAL

Two epitaxial films each of Tl-2212 (6000-Å thick) and Tl-2223 (4300-Å thick) on $LaAlO_3$ (100) substrates are obtained by sputter deposition of Tl-free precursor films followed by an *ex situ* anneal together with Tl-rich Tl-2223 pellets in an alumina crucible for thallination. Details of the film growth, annealing, and characterization are described elsewhere.[27] The zero-resistance temperatures of the Tl-2223 films are 112.5 and 114 K, and the Tl-2212 films have Meissner transitions at 102 K as determined with a superconducting quantum interference device magnetometer. Five 1-μm thick epitaxial films of (Tl, Bi)-1223 are grown on $LaAlO_3$ (100) substrates by laser ablation, followed by post-growth annealing of the films wrapped in Ag foil together with Tl-rich (Tl, Bi)-1223 pellets. This procedure typically yields films with zero-resistance temperatures in the range 105–111 K. Details of the film growth, annealing, and characterization are described elsewhere.[28,29] Epitaxial films of the rare earth cuprates La_2CuO_4, Nd_2CuO_4, and Gd_2CuO_4 are grown by pulsed laser deposition in 100 mTorr background pressure of oxygen onto $LaAlO_3$ (100) substrates at 650 °C.

The film surfaces are cleaned in a dry box with an inert ultrahigh purity N_2 atmosphere which encloses the load lock area of the XPS spectrometer using a nonaqueous etchant consisting of 0.1% Br_2 in absolute ethanol for 15–60 sec (etch rate ~1000 Å/min), rinsed in ethanol, and loaded into the XPS spectrometer with no atmospheric exposure. The XPS spectrometer is a Surface Science Instruments SSX-501 utilizing monochromatic Al K_α x-rays (1486.6 eV). Spectra are measured at ambient temperature with photoemission normal to the surface. The core level spectra are measured with an x-ray spot size of 150 μm and the pass energy of the electron energy analyzer is set to 25 eV. The energy scale is calibrated using sputter-cleaned Au and Cu with the Au $4f_{7/2}$ binding energy set to 83.95±0.05 eV [0.7 eV full width at half-maximum (FWHM)] and the Cu $2p_{3/2}$ binding energy set to 932.45±0.05 eV (1.0 eV FWHM). The surface preparation, XPS spectrometer characteristics, and measurement conditions are described in more detail elsewhere.[2,7]

The measured surface stoichiometries normalized to Cu are Tl:Ba:Ca:Cu:O=1.65:2.1:2.25:3 for the Tl-2223 films, Tl:Ba:Ca:Cu:O=2:2.2:1.2:2 for the Tl-2212 films, and Tl:Bi:Sr:Ba:Ca:Cu:O=0.8:0.3:1.6:0.5:1.8:3 for the (Tl, Bi)-1223 films. The slight deviations from the expected bulk stoichiometries may result from residual surface and/or grain boundary contaminants, evident in the XPS spectra as residual high binding energy signals in the O 1*s* and alkaline earth core level regions, or from the layered nature of these materials, since the *c*-axis lattice constants are comparable to or greater than typical photoelectron attenuation lengths. The (Tl, Bi)-1223 films have an Ag contaminant present at a level of 1–2 at.%, presumably from the annealing procedure, which contributes a detectable small feature to the valence band spectra, as discussed later.

After completion of the XPS measurements, ac susceptibility determinations of T_c (typically slightly lower than zero-resistance temperatures) were performed. The measured onsets of the superconducting transition temperature and transition widths ΔT_c for the Tl-2223 films are T_c=109 and 111 K and ΔT_c=2 K, T_c=103–106 K and ΔT_c=1 K for the (Tl, Bi)-1223 films; and T_c=102 and 104 K and ΔT_c=1 K for the Tl-2212 films.

III. RESULTS AND DISCUSSION

The results of the XPS measurements of core levels other than the Cu 2*p* are summarized in Table I for 16 samples of the 5 different Tl cuprate phases measured in this lab, as well as previous measurements in this lab[30] for epitaxial films of $HgBa_2CaCu_2O_{6+\delta}$ (Hg-1212), which is chemically and structurally closely related to the Tl cuprates. The core level binding energies are determined from least squares fitting for the Tl 4*f* and Ba 3*d* and 4*d* signals, which consist of a single component or which contain components which are well separated. For the Ca 2*p* and O 1*s* signals, which consist of components with significant overlap, the uncertainty in the least squares fitting is considerably greater, with the determined binding energies varying by as much as 0.2 eV (but typically <0.1 eV) for the same spectrum with different initial fitting parameters. The binding energies for these core levels listed in Table I are therefore those determined from the second derivatives, for which the variability is generally comparable to the other core levels.

XPS measurements of the Cu 2*p* core levels for the Tl and rare earth cuprates are summarized in Table II, together with previous measurements in this lab for Hg-1212 (Ref. 30), $Bi_2Sr_2CaCu_2O_8$ (Bi-2212),[31] and $YBa_2Cu_3O_7$ (Y-123).[32] The Cu $2p_{3/2}$ satellite to main peak intensity ratios (I_s/I_m) are determined from the integrated intensities above a flat background from the smoothed spectra, and the positions listed in Table II are the centroids. The data in Tables I and II show that the measurements from different films of the same phase with similar T_c's are very similar, demonstrating good sample-to-sample reproducibility. The results for Tl-2212 are similar to previous measurements in this lab using films grown with a different technique and different photoemission measurement conditions.[33,34]

The O 1*s* spectra for the five Tl cuprate phases considered here are shown in Fig. 1. The signal near 531 eV is dominant prior to etching and is associated with contaminants, particularly hydroxides and carbonates of the reactive alkaline earth elements.[35] The lower binding energy manifold near 528 eV consists of signals from the inequivalent lattice sites in the superconductors. This signal is clearly detectable prior to etching and the binding energy is not affected by the etching (as is also the case for the other core levels), an indication that the surface is not detectably damaged by the etching. The dominance of the lower binding energy signals evident in Fig. 1 is a measure of the surface quality achieved in this work. In earlier works on Tl cuprates, the O 1*s* signals were

TABLE I. Summary of core level binding energies and peak full widths at half maximum (in parentheses) for (Tl, Bi)-1223, Tl-2212, and Tl-2223 epitaxial films measured in this work, together with previously reported measurements from this lab for epitaxial films of Tl-2201, Tl-1212, and Hg-1212.

Material	T_c	Tl $4f_{7/2}$	Ba $3d_{5/2}$	Ba $4d_{5/2}$	Ca $2p_{3/2}$	O 1s	Source
Tl-1212	87.5	117.75 (1.42)	778.09 (1.51)	87.67 (1.20)	344.42 and 345.51	528.08 and 528.58	Ref. 2
	86.4	117.83 (1.42)	778.13 (1.50)	87.71 (1.14)	344.45 and 345.65	527.99 and 528.55	Ref. 2
(overdoped)	74.5	117.66 (1.40)	777.99 (1.48)	87.56 (1.18)	344.40 and 345.49	527.93 and 528.55	Ref. 2
(Tl, Bi)-1223	106.1	117.83 (1.33)	777.94 (1.44)	87.56 (1.11)	344.59 and 345.73	527.98 and 528.51	This work
	105.3	117.81 (1.32)	777.92 (1.45)	87.55 (1.05)	344.61 and 345.70	528.02 and 528.61	This work
	105.2	117.83 (1.34)	777.94 (1.48)	87.57 (1.05)	344.64 and 345.72	528.01 and 528.62	This work
	104.7	117.79 (1.29)	777.92 (1.47)	87.56 (1.08)	344.59 and 345.37	528.01 and 528.63	This work
	103.2	117.82 (1.30)	777.97 (1.48)	87.57 (1.07)	344.65 and 345.53	528.01 and 528.56	This work
Tl-2201	63	118.12 (1.25)	777.89 (1.44)	87.50 (1.05)	none	527.50 and 528.95	Ref. 7
	53	118.20 (1.27)	778.00 (1.51)	87.61 (1.20)	none	527.57 and 528.97	Ref. 7
(overdoped)	11	117.88 (1.23)	777.77 (1.49)	87.35 (1.03)	none	527.39 and 528.63	Ref. 7
(overdoped)	11	117.86 (1.19)	777.76 (1.45)	87.36 (1.04)	none	527.39 and 528.58	Ref. 7
Tl-2212	104.2	117.98 (1.27)	778.26 (1.47)	87.89 (1.11)	344.57 and 345.67	527.97 and 528.75	This work
	101.8	118.03 (1.27)	778.34 (1.48)	87.96 (1.17)	344.64 and 345.89	527.95 and 528.80	This work
Tl-2223	111.4	117.84 (1.23)	778.05 (1.43)	87.67 (1.11)	344.61 and 345.78	527.94 and 528.63	This work
	109	117.91 (1.21)	778.10 (1.43)	87.71 (1.06)	344.58 and 345.80	527.96 and 528.73	This work
Hg-1212	117	none	778.21 (1.44)	87.83 (1.13)	344.39 and 345.58	527.82 and 528.70	Ref. 30
	116	none	778.28 (1.52)	87.96 (1.15)	344.47 and 345.56	527.86 and 528.69	Ref. 30

TABLE II. Summary of the Cu $2p_{3/2}$ main peak binding energies (E_m = centroid position), peak full widths at half maximum (FWHM), satellite-main peak intensity ratios (I_s/I_m), and satellite-main peak energy separations ($E_s - E_m$) for epitaxial films of the Tl and rare earth cuprate phases measured in this work, together with previously reported measurements from this lab.

Material	T_c	E_m	FWHM	I_s/I_m	$E_s - E_m$	Source
Tl-1212	87.5	933.53	3.39	0.419	8.47	Ref. 2
	86.4	933.49	3.44	0.418	8.47	Ref. 2
	74.5 (overdoped)	933.51	3.49	0.425	8.46	Ref. 2
(Tl, Bi)-1223	106.1	933.45	3.71	0.374	8.55	This work
	105.3	933.42	3.68	0.372	8.54	This work
	105.2	933.42	3.64	0.374	8.51	This work
	104.7	933.48	3.39	0.379	8.44	This work
	103.2	933.47	3.49	0.376	8.47	This work
Tl-2201	63	933.34	3.35	0.450	8.46	Ref. 7
	53	933.33	3.31	0.421	8.54	Ref. 7
	11 (overdoped)	933.36	3.39	0.476	8.49	Ref. 7
	11 (overdoped)	933.33	3.35	0.446	8.41	Ref. 7
Tl-2212	104.2	933.45	3.50	0.397	8.44	This work
	101.8	933.56	3.49	0.413	8.34	This work
Tl-2223	111.4	933.41	3.53	0.391	8.46	This work
	109	933.38	3.45	0.376	8.52	This work
Hg-1212	117	933.41	3.72	0.362	8.63	Ref. 30
	116	933.50	3.72	0.371	8.55	Ref. 30
Bi-2212	85	933.48	3.50	0.413	8.58	Ref. 31
Y-123	89	933.39	3.50	0.407	8.41	Ref. 32
	0 (underdoped)	933.47	2.40	0.289	8.78	Ref. 32
La_2CuO_4	0	933.51	2.93	0.411	8.73	This work
Nd_2CuO_4	0	933.75	3.39	0.363	9.01	This work
Gd_2CuO_4	0	934.19	3.15	0.388	8.73	This work

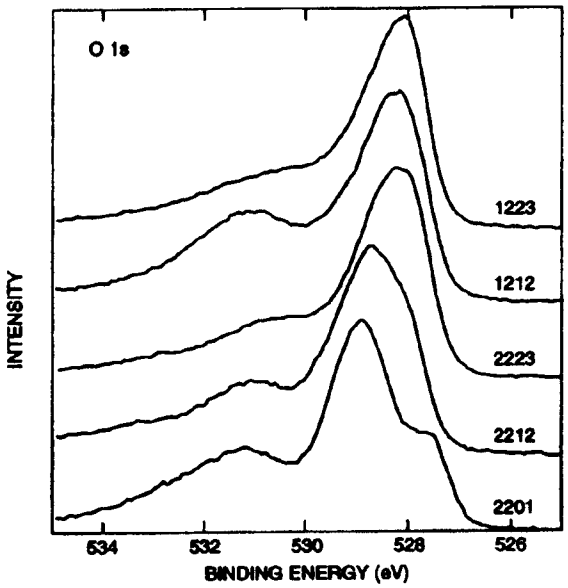

FIG. 1. Representative O 1s spectra measured from the five Tl cuprate phases considered in this work.

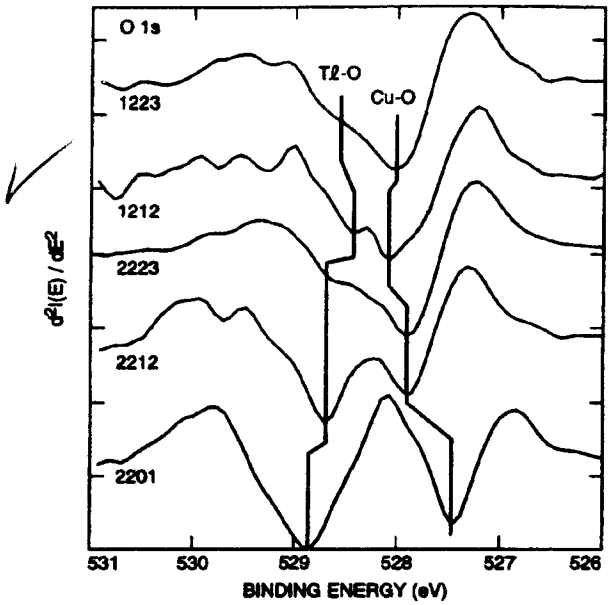

FIG. 2. Second derivatives of the spectra from Fig. 1, showing more clearly the two components of the spectra associated with Cu-O and Tl-O bonding.

either not reported,[19–21] making an assessment of the intrinsic nature of the measurements problematic, or the higher binding energy contaminant signals were significantly larger[23,24] than those evident in Fig. 1.

A. Cu-O bonding

Information on the Cu-O bonding can be obtained from the O 1s and Cu 2p core levels. The low binding energy O 1s signal consists of two components, most clearly evident in the Tl-2201 spectrum (bottom curve in Fig. 1), associated with Cu-O bonding (lowest binding energy component) and Tl-O bonding (~1 eV higher binding energy). The two components are more clearly separated in the second derivatives shown in Fig. 2. The differing line shapes evident in Fig. 1 result from differences in the energy separations of these two components (see Fig. 2) and from differences in the relative intensities due to the differing Tl/Cu ratios in the various phases. A qualitative understanding of the observed O 1s binding energies and their relationship to chemical bonding can be gained by consideration of the crystal structures of the various Tl cuprate phases.[8–12] To avoid confusion related to the different atom numbering employed for the various phases, the Cu-O planar oxygen in the single and double Cu-O layer materials and in the outer Cu-O layers of triple Cu-O layer materials will be referred to as O(1), the Cu-O planar oxygen in the middle Cu-O layer of triple Cu-O layer materials will be referred to as O(1′), the apical oxygen (Ba-O layers) will be referred to as O(2), and oxygen in the Tl-O layers will be referred to as O(3).

In addition to in-plane coordination to two Cu atoms, each O(1) is coordinated to either four Ba^{2+} ions (Tl-2201) or two Ba^{2+} and two Ca^{2+} ions (Tl-n212 and the outer Cu-O planes in Tl-n223) and each O(1′) is coordinated to four Ca^{2+} ions. There appears to be no correlation of the O 1s binding energies and the Cu-O bond lengths, which for the Tl cuprates considered here are all near 1.93 Å with the exception of (Tl, Bi)-1223 which has Cu-O bond lengths of 1.91 Å. However, as shown in Fig. 3, O(1,1′) O 1s binding energies are correlated with the much longer Ba-O(1) bond lengths (2.73–2.84 Å, due to the larger Ba^{2+} ionic radius), with lower O 1s binding energies occurring for shorter Ba-O(1) bond lengths. Since the (Ba, Sr)-O(1) bond length determined by powder neutron diffraction[12] in (Tl, Bi)-1223 is an average, the local Ba-O(1) bond length is assumed to be the same as in Tl-1223 (Ref. 11). Also included in Fig. 3 is Hg-1212 using previously reported XPS measurements from this lab[30] and the crystal structure reported in the literature.[36]

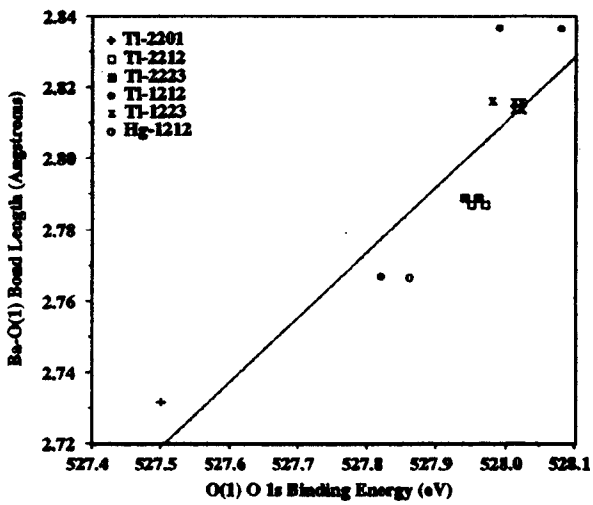

FIG. 3. Ba-O(1) bond length vs O 1s binding energy, using the data from Table I for those samples near optimum doping and crystal structure determinations from the literature (Refs. 8–12, 36). A linear least squares fit is also shown as a guide to the eye.

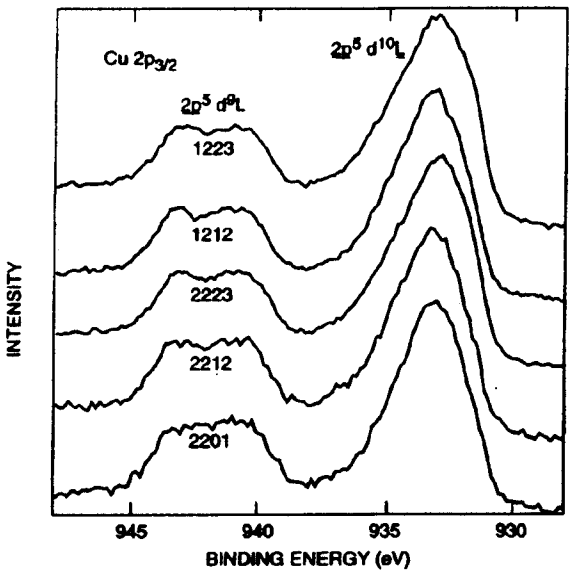

FIG. 4. Representative Cu $2p_{3/2}$ spectra measured from the five Tl cuprate phases considered in this work.

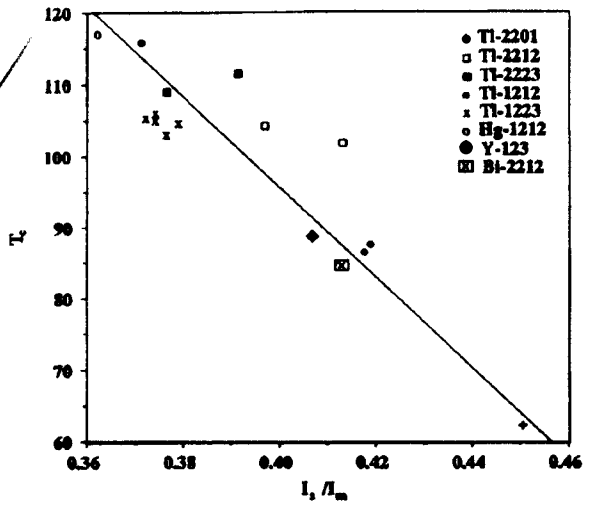

FIG. 5. T_c vs I_s/I_m, using the data from Table II for those samples near optimum doping. A linear least squares fit is also shown as a guide to the eye.

Contributions to a lower O 1s binding energy resulting from a shorter Ba-O(1) bond length include an increased Madelung energy at the O(1) site (assuming other contributions to the Madelung energy remain constant) and increased polarization screening of the photoionized O 1s core hole final state. If the effect of the alkaline earth-O(1) bond length on the Madelung energy is the dominant effect, then one would expect that the O 1s binding energy for Tl-2201 [four Ba-O(1) bonds] would be higher than for the other Tl cuprates [two Ba-O(1) and two Ca-O(1) bonds, or four Ca-O(1′) bonds], since the Ca-O(1,1′) bond lengths are much shorter than the Ba-O(1) bond lengths. This is the opposite of what is observed. Alternatively, if the polarization screening is the dominant effect, then the O 1s binding energy for Tl-2201 would be lower than for the other Tl cuprates, which is consistent with the measurements presented here, since the polarizability of Ba^{2+} is more than triple that of Ca^{2+} (Ref. 37). Though not conclusive, the correlation evident in Fig. 3 thus suggests that the final state screening is the dominant contributor to the observed differences in the O 1s binding energies evident in Figs. 2 and 3.

Representative Cu $2p_{3/2}$ spectra are presented in Fig. 4. The multiplet at higher binding energy, referred to as a satellite peak in the literature, corresponds to states of predominant $2p^5 3d^9\underline{L}$ character, where underscoring denotes a hole and $\underline{L}$ is the oxygen ligand, while the main peak at lower binding energy corresponds to states of predominant $2p^5 3d^{10}\underline{L}$ character resulting from ligand-to-metal (O $2p \rightarrow$ Cu $3d$) charge transfer.[14,17,38] It is to be noted that the values of I_s/I_m in Table II are at the high end of the range of values found in the literature, e.g., for Tl-2223 the value of 0.38–0.39 in this work compares to previously reported values of 0.19 (Ref. 20), 0.24 (Refs. 19, 21), 0.21 and 0.38 (Ref. 24), and 0.38 (Ref. 23). The variability in reported results is likely due to problems in reproducibly obtaining high quality surfaces, since typically surface preparation consists of scraping a polycrystalline pellet in vacuum, which has been reported to cause reduction of Cu^{2+} to Cu^{1+} (i.e., low values of I_s/I_m) for other cuprate superconductors.[35,39,40]

As shown in Fig. 5, higher values of T_c are correlated with lower values of I_s/I_m for samples near optimum doping. This trend is consistent with some earlier reports,[20,21] despite the differences in reported values of I_s/I_m, and is in contradiction to other studies.[18,19] We now consider factors which may explain such a correlation. As previously mentioned, I_s/I_m and $E_s - E_m$ are related to the parameters Δ (O $2p \rightarrow$ Cu $3d$ charge transfer energy), T (Cu $3d$-O $2p$ hybridization energy), and U (on-site Coulomb interaction between Cu $2p$ and $3d$ holes) in a simple configuration interaction model.[14–17] Although the two experimentally determined quantities are insufficient to uniquely determine the three model parameters, the data set in Table II is sufficient to restrict their values to narrow ranges. The experimental values of I_s/I_m and $E_s - E_m$ in Table II for all of the superconducting cuprates are reproduced in calculations for $\Delta = 0.5$–1.0 eV, $T = 2.2$–2.5 eV, and $U = 7.6$–8.0 eV. If the oxygen-oxygen interaction is included in the calculations and fixed at 0.5 eV, as in Ref. 15, then $\Delta = -0.5$ to 0 eV. This range of values for Δ corresponds to Cu d orbital occupancy $n_d \sim 9.4$, characteristic of strong mixed valency as previously noted.[15]

Comparison of the measured values of I_s/I_m and $E_s - E_m$ with the values calculated as Δ or T is varied with the other two model parameters fixed is shown in Fig. 6. Decreasing values of I_s/I_m and increasing values of $E_s - E_m$ are reasonably well explained qualitatively by calculations with either decreasing values of Δ or increasing values of T, i.e., more covalent Cu-O bonding. T is to first order proportional to $d_{\text{Cu-O}}^{-4}$ (Ref. 17), where $d_{\text{Cu-O}}$ is the Cu-O bond length. Since the Tl cuprates, as well as Hg-1212, have very similar Cu-O bond lengths, then variation of Δ is likely to be the dominant cause of changes in I_s/I_m and $E_s - E_m$. The correlation evident in Fig. 5 therefore suggests that higher values of T_c are related to low values of the O $2p \rightarrow$ Cu $3d$ charge transfer energy.

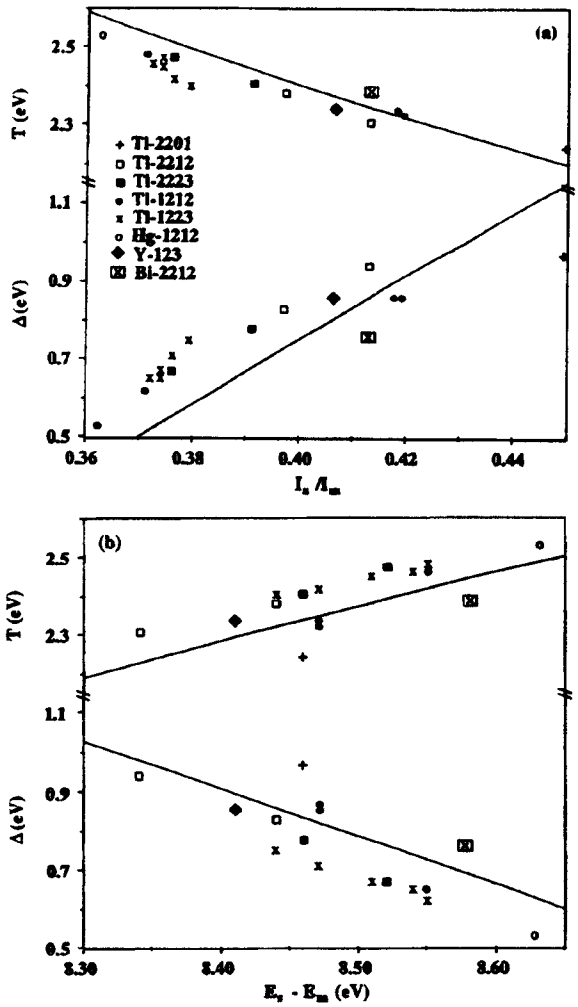

FIG. 6. Plots of T and Δ vs (a) I_s/I_m and (b) E_s-E_m. The curves are the calculated values of I_s/I_m and E_s-E_m as (top curve in each panel) T is varied for fixed Δ (0.75 eV) and U (7.8 eV), and (bottom curve in each panel) Δ is varied for fixed T (2.4 eV) and U (7.8 eV). The data points are the experimental values of I_s/I_m and E_s-E_m vs the values of T or Δ obtained from the individual spectra.

Finally, we consider the effects of differences in oxygen coordination on the Cu-O bonding as reflected in the Cu $2p$ spectra. In studies comparing the Cu $2p$ spectra measured from La_2CuO_4 (distorted octahedral O coordination to Cu) and Nd_2CuO_4 (square planar coordination), it has been reported that in the latter compound the main line is narrower.[13] The proposed explanation was that O $2p_{x,y}$ $\rightarrow$Cu $3d_{x^2-y^2}$ charge transfer occurs in both compounds, while O $2p_z\rightarrow$Cu $3d_{z^2}$ charge transfer is possible only in La_2CuO_4. The additional charge transfer pathway results in an additional contribution to the main peak, and thus a broader and asymmetric signal, as is also observed in high temperature superconductors. To verify this, measurements on La_2CuO_4, Nd_2CuO_4, and Gd_2CuO_4 (which has the Nd_2CuO_4 crystal structure and square planar O coordination to Cu) have been done in this work, and the results are included in Table II. A possible problem with the scenario

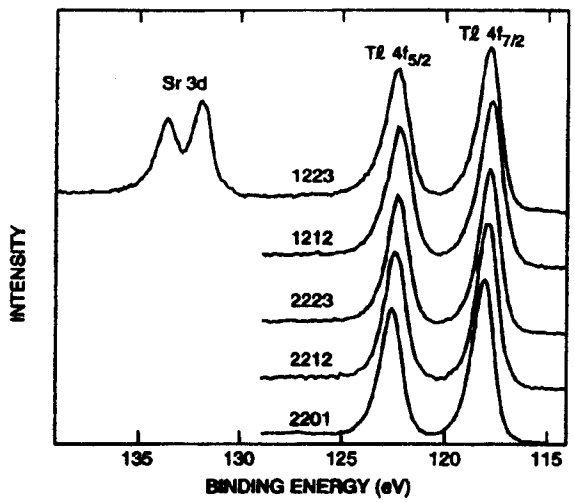

FIG. 7. Representative Tl $4f$ spectra measured from the five Tl cuprate phases considered in this work.

described above is that, in the absence of other differences, with the additional charge transfer one might also expect I_s/I_m to be lower for La_2CuO_4, while the opposite is observed in this work as well as in earlier studies.[17,41,42] Among the Tl cuprates, Tl-2201 with octahedral coordination also exhibits a higher value of I_s/I_m compared to the other cuprates which have pyramidal or mixed pyramidal and square planar coordination (see Table II). The measured widths of the Cu $2p$ main peaks are also larger for Nd_2CuO_4 and Gd_2CuO_4 than for La_2CuO_4, which is also contrary to expectations based on the model described above. The suggestion that the peak shapes of the main Cu $2p$ signals reflect the specific suggested differences in charge transfer pathways therefore does not appear to be supported by the measurements in this work.

B. Tl-O bonding

Information on the Tl-O bonding can be obtained from the Tl $4f$ spectra and the higher binding energy component of the O $1s$ spectra. Representative Tl $4f$ spectra measured from each of the five Tl cuprate phases measured in this lab are presented in Fig. 7. The spectra are well represented by a single doublet in the expected 4:3 intensity ratio, consistent with a single Tl chemical state. The higher binding energy component of the O $1s$ spectra originates from Tl-O bonds, which are to O(2,3)p_z states as discussed below.

Crystal structure determinations[8–12] show that the in-plane Tl-O(3) distances are much longer than Tl-O distances in the c direction, which are Tl bonds to the O(2) (apical) oxygens, and in the case of the double Tl-O layer materials also to O(3) in the adjacent Tl-O layers. Band structure calculations[2,43,44] also show that the in-plane Tl-O(3) $p_{x,y}$ interactions are weak, while the stronger Tl $6s$-O(2,3)p_z covalent interactions yield hybridized states. For the double Tl-O layer materials, the hybridized states form occupied bonding bands of predominant Tl $6s$ character which are ~7 eV below the Fermi energy, and antibonding bands of predominant O(2,3)p_z character which are ~0–2 eV above the Fermi level and are nearly empty, but do dip slightly below

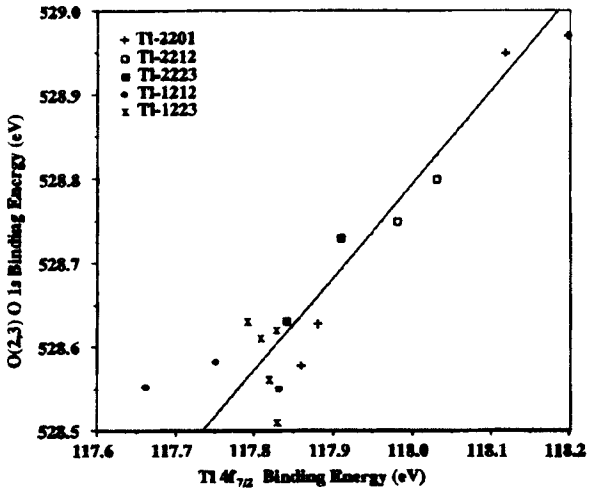

FIG. 8. O(2,3) $O\,1s$ vs Tl $4f_{7/2}$ binding energies. A linear least squares fit is also shown as a guide to the eye.

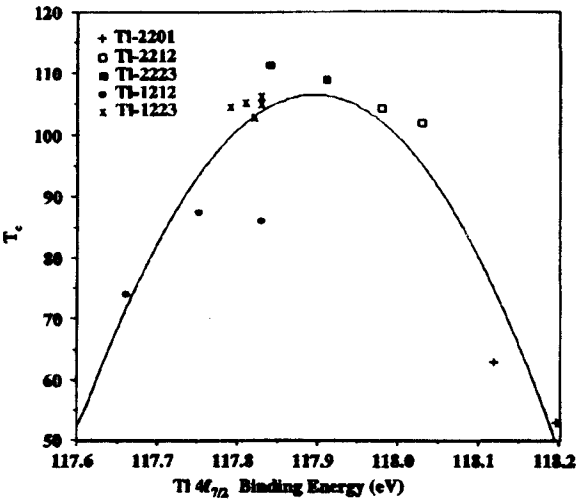

FIG. 9. T_c vs the Tl $4f_{7/2}$ binding energy for samples near optimum doping. A quadratic least squares fit is also shown as a guide to the eye.

the Fermi level forming electron pockets at the Γ point, and also at the Z point for Tl-2212 and Tl-2223. For the single Tl-O layer materials the situation is similar, but both the bonding and antibonding bands are ~2 eV higher energy (lower binding energy) so that the antibonding bands are completely empty. In all cases states with significant Tl $6s$ character are therefore occupied, so Tl should be viewed as mixed valent and in terms of formal oxidation state is intermediate between Tl^{1+} and Tl^{3+}. However, Tl should not be viewed as discrete ions, some with occupied and some with empty $6s$ orbitals, since the bands are dispersive and the electrons are thus delocalized.

Higher Tl $4f_{7/2}$ binding energies are correlated with higher O(2,3) O $1s$ binding energies, as shown in Fig. 8. Data from both near-optimally doped and overdoped Tl-2201 and Tl-1212 are included in Fig. 8, and for these materials a linear correlation is not surprising since variation in doping causes a shift in the chemical potential which is observable as a rigid shift of all core levels. The observed slope near unity even when only optimally doped samples are considered suggests that the correlation may also reflect differences in the chemical potential between materials. However, the other core levels do not shift rigidly with the Tl $4f_{7/2}$ core level, e.g., the near-optimally doped Tl-2201 samples exhibit the highest Tl $4f_{7/2}$ binding energies but the lowest Cu $2p_{3/2}$ binding energies among the phases studied, and comparing Tl-2201 with Tl-2212 the Tl $4f_{7/2}$ binding energies are the most similar among the phases studied, while the Ba core level binding energies are the most dissimilar. Therefore, other effects need to be considered.

Usually a higher metal core level binding energy indicates increased metal-to-ligand charge transfer and should be correlated with lower ligand core level binding energies. However, the higher Tl core level binding energies of Tl^{1+} compounds relative to Tl^{3+} compounds are well documented,[19,25,45,46] and have been attributed to enhanced final state relaxation in conductive Tl^{3+} compounds,[45] though specific calculations or additional experimental evidence in support of this conjecture appear to be lacking. The data in Fig. 8 thus seem to be consistent with the view[19,21–23,25,26] that the Tl $4f_{7/2}$ binding energies in Tl cuprates reflect mixed valent Tl (which is also consistent with band structure calculations), with single Tl-O layer materials being closest to Tl^{3+}. However, states with predominant Tl $6s$ character in the single Tl-O materials remain well below the Fermi level and hence are occupied and the formal oxidation state remains intermediate between Tl^{1+} and Tl^{3+}. The observed variation of the Tl core level binding energies for the various phases may reflect differences in the occupation of the Tl $6s$ states, or differences in the relative Tl $6s$ character of the states.

Finally, for samples which are reasonably close to optimum doping we note a correlation between the Tl $4f_{7/2}$ binding energy and T_c, with maximum T_c occurring for Tl $4f_{7/2}$ binding energies near 117.9 eV, as shown in Fig. 9. This correlation is not evident for samples far from optimum doping, e.g., overdoped Tl-2201 ($T_c = 11$ K) also exhibits Tl $4f_{7/2}$ binding energies near 117.9 eV. The correlation evident in Fig. 9 appears similar in form to the correlation observed in a study[47] of the effect of pressure on Tl-2212, in which T_c was found to be maximum for an optimum Ba z coordinate. Indeed, comparing the crystal structures of the various Tl cuprate phases[8–11] shows that T_c is maximum for a Ba-O(3) distance near 2.85 Å, suggesting a relationship between the Ba-O(3) bond length and the Tl $4f_{7/2}$ binding energy. This conjecture is confirmed in Fig. 10. The correlation evident in Fig. 10 is not surprising for double Tl-O layer materials, since Tl is bonded to O(3) atoms in the adjacent Tl-O layers. However, in single Tl-O layer materials, the only Tl-O(3) interactions are the weak in-plane interactions, which suggests that other factors may be responsible, such as the Madelung energy or that charge transfer between the Tl-O and Cu-O layers is mediated by the Ba^{2+} ions.

C. Alkaline earth-oxygen bonding

Representative Ba $4d$ spectra measured from the five Tl cuprate phases considered in this work are presented in Fig.

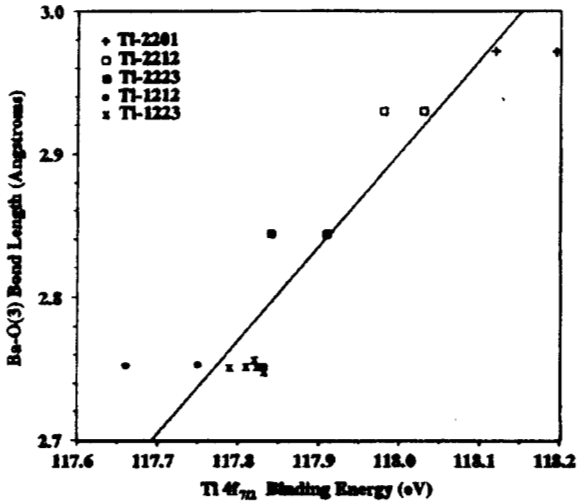

FIG. 10. Ba-O(3) bond length vs the Tl $4f_{7/2}$ binding energy for samples near optimum doping. A linear least squares fit is also shown as a guide to the eye.

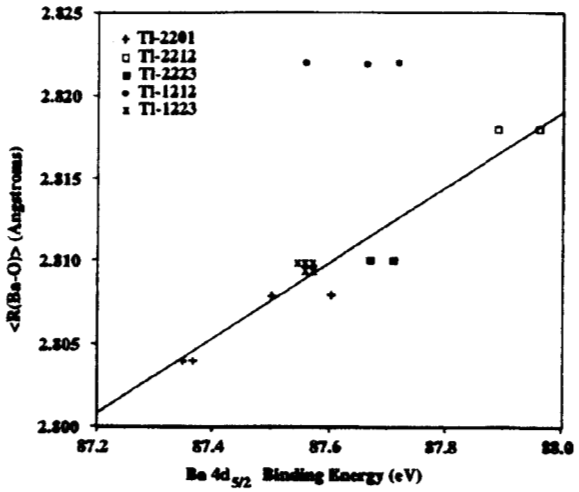

FIG. 12. The average Ba-O bond length $\langle R(\text{Ba-O})\rangle$ vs the Ba $4d_{5/2}$ binding energy. The line is a guide to the eye.

11. Each spectrum consists of a dominant doublet at low binding energy corresponding to the superconducting phase, and a minor doublet at higher binding energy corresponding to residual surface contaminant phases. The spectra are consistent with Ba being in a single chemical state, and are comparable to Ba $4d$ signals measured from other cuprate superconductors (e.g., see the review in Ref. 48).

Ba is coordinated to four O(1) atoms, four O(2) atoms, and one O(3) atom. Band structure calculations[2,43,44] show that the valence band states have little Ba or Ca character; to a good approximation the alkaline earths can therefore be considered to be ideally ionic. As previously noted, the O(1,1′) O $1s$ binding energies are correlated with the Ba-O(1) bond lengths (Fig. 3), and the Tl $4f_{7/2}$ binding energies are correlated with the Ba-O(3) bond lengths (Fig. 10). The Ba $4d_{5/2}$ binding energies, on the other hand, do not correlate with any individual Ba-O bond length. However, a reasonable correlation with the average Ba-O bond length $\langle R(\text{Ba-O})\rangle$ is evident, as shown in Fig. 12, with lower $\langle R(\text{Ba-O})\rangle$ corresponding to lower Ba $4d_{5/2}$ binding energies, though a larger deviation from the trend line is apparent for data measured from Tl-1212 samples compared to data measured from the other Tl cuprate phases. The observed trend is consistent with both the increased Madelung energy and with increased polarization screening of the Ba^{2+} ions with smaller Ba-O bond lengths. While both effects are expected to contribute to the observations, previous studies of simple alkaline earth salts have shown that the Madelung energy is the dominant factor.[49–51]

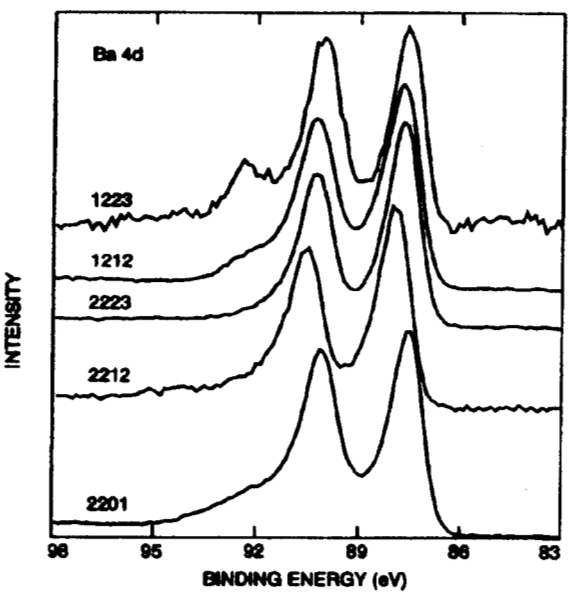

FIG. 11. Representative Ba $4d$ spectra measured from the five Tl cuprate phases considered in this work.

Representative Ca $2p$ spectra measured from the four Ca-containing Tl cuprate phases considered in this work are presented in Fig. 13. Each spectrum consists of two doublets separated by approximately 1 eV. Both of these components occur at significantly lower binding energies than the signal from surface contaminants (Ca $2p_{3/2}$ binding energy near 347 eV), which is prominent prior to etching but is not detectable in the spectra in Fig. 13. These spectra are comparable to Ca $2p$ signals measured from other Ca-containing cuprate superconductors (e.g., see the review in Ref. 48), and the two signals have been interpreted as originating from occupation of inequivalent lattice sites due to cation disorder, with the lower binding energy component corresponding to the site between Cu-O planes. Significant cation disorder has in fact been detected in structure studies of Tl cuprates.[52,53]

Ca^{2+} ions are coordinated to eight O(1) atoms in double Cu-O layer Tl cuprates, and to four O(1) and four O(1′) atoms in triple Cu-O layer Tl cuprates. There is relatively little variation in the Ca $2p_{3/2}$ binding energies between the various Tl cuprate phases, reflecting the similarity of the chemical environments since the average Ca-O bond distance is 2.48 ± 0.01 Å for all of the Ca-containing Tl cuprates studied here.

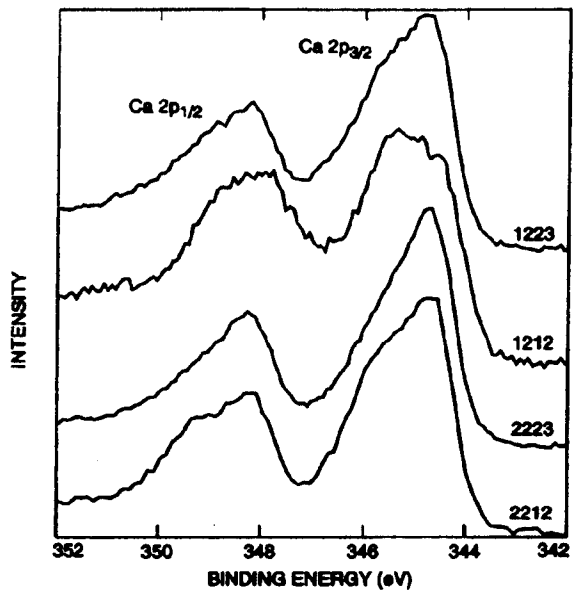

FIG. 13. Representative Ca $2p$ spectra measured from the four Ca-containing Tl cuprate phases considered in this work.

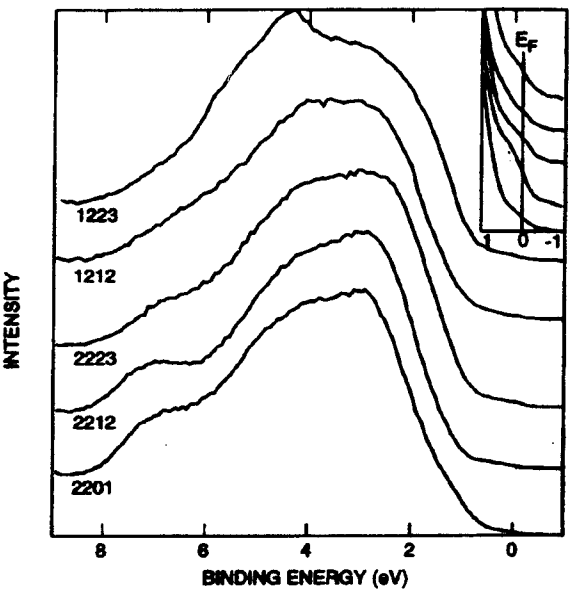

FIG. 14. Representative valence band spectra measured from the five Tl cuprate phases considered in this work. Inset: Fermi level region.

The Ba and Ca core level binding energies measured from the Tl cuprates are significantly lower than those measured from the corresponding metals, as is also the case for other cuprate superconductors[48] and simpler alkaline earth compounds.[49] The negative chemical shift observed in alkaline earth compounds is attributable to initial-state electrostatic effects, originating from the larger value of the Madelung energy relative to the ionization energy.[49–51]

D. Valence band measurements

Representative valence band spectra measured from the five Tl cuprate phases considered in this work are presented in Fig. 14. A closer view of the Fermi level region is shown in the inset of Fig. 14. The density of states at the Fermi level for the Tl cuprates is lower than is observed for other cuprate superconductors (e.g., see the review in Ref. 35), though Fermi edges are still apparent with varying degrees of clarity. The intensity of the feature near 4.5 eV in the spectrum measured from (Tl, Bi)-1223 correlates with the level of Ag contaminant observed on the surface, and is thus an artifact of the annealing procedure.

The valence bands are comprised of states with primarily Cu $3d$, O $2p$, and Tl $6s$ and $5d$ character.[2,43,44] For the photon energy used in this work, the photoionization cross sections are such that the Cu and Tl states are dominant in the spectra.[54,55] The feature near 7 eV consists of states with primarily Tl $6s$ character.[2,43,44,55] The variation in the relative intensity of this feature, evident in Fig. 14, is consistent with the variation in the Tl/Cu ratios in the phases studied here. The main manifold in the 1–6 eV region consists of states with primarily Cu $3d$ character and exhibits relatively little difference for the various phases, reflecting the similarity in the calculated Cu $3d$ partial densities of states.[2,43,44]

IV. SUMMARY AND CONCLUSIONS

Photoemission measurements of Tl-2212, Tl-2223, and Tl, Bi-1223 have been presented which, together with previous measurements in this lab of Tl-2201 (Ref. 7) and Tl-1212 (Ref. 2), comprise a comprehensive data set for a comparative study of Tl cuprates with a range of chemical and electronic properties. Higher values of T_c have been found to correlate with low values of I_s/I_m and high values of $E_s - E_m$ in the Cu $2p$ spectra. Analysis of these spectra within a simple configuration interaction model suggests that higher values of T_c are related to low values of the O $2p \rightarrow$ Cu $3d$ charge transfer energy, i.e., to more covalent Cu-O bonding. In the O $1s$ region, a smaller Ba-O(1) bond length has been found to correlate with a lower binding energy for the signal associated with Cu-O bonding, most likely resulting from the increased polarization screening by Ba^{2+} ions. For samples near optimum doping, maximum T_c has been observed to occur when the Tl $4f_{7/2}$ binding energy is near 117.9 eV, which is near the middle of the range of values observed for Tl cuprates. Higher Tl $4f_{7/2}$ binding energies, corresponding to formal oxidation states nearer Tl^{1+}, have also been found to correlate with longer Ba-O(3) bond lengths and higher binding energies of the O $1s$ signal associated with Tl-O bonding. The alkaline earth core levels have been found to be similar to those measured from other cuprate superconductors. The measured valence bands have been found to be very similar to each other, consistent with the similarity in the Cu $3d$ partial densities of states found in band structure calculations, with the exception of a feature near 7 eV corresponding to states with predominant Tl $6s$ character, the relative intensity of which varies consistently with the varying Tl/Cu ratio in the phases studied.

ACKNOWLEDGMENTS

Part of the work described in this paper was performed by the Center for Space Microelectronics Technology, Jet Pro-

pulsion Laboratory, California Institute of Technology, and was sponsored by the National Aeronautics and Space Administration, Office of Space Science. Part of this work was performed at Sandia National Laboratories, Albuquerque, NM, and supported by the U.S. Department of Energy, Office of Basic Energy Sciences under Contract No. DE-ACO4-94AL85000. The work performed at SUNY at Buffalo was supported partially by the U.S. Department of Energy, Office of Basic Energy Sciences under Grant No. DE-FG02-98ER45719 and Oak Ridge National Laboratory.

*Electronic address: richard.vasquez@jpl.nasa.gov

[1] D. L. Novikov and A. J. Freeman, in *Recent Advances in High Temperature Superconductivity*, edited by J. Klamut, B. W. Veal, B. M. Dabrowski, P. W. Klamut, and M. Kazimierski, Vol. 475 of *Lecture Notes in Physics* (Springer-Verlag, New York, 1996).

[2] R. P. Vasquez, D. L. Novikov, A. J. Freeman, and M. P. Siegal, Phys. Rev. B **55**, 14 623 (1997).

[3] M. P. Siegal, E. L. Venturini, P. P. Newcomer, B. Morosin, D. L. Overmyer, F. Dominguez, and R. Dunn, Appl. Phys. Lett. **67**, 3966 (1995).

[4] N. H. Hur, N. H. Kim, K. W. Lee, K. H. Yoo, Y. K. Park, and J. C. Park, Physica C **234**, 19 (1994).

[5] N. H. Hur, M. Paranthaman, J. R. Thompson, and D. K. Christen, Physica C **268**, 266 (1996).

[6] S. Nakajima, M. Kikuchi, Y. Syono, N. Kobayashi, and Y. Muto, Physica C **168**, 57 (1989).

[7] R. P. Vasquez, Z. F. Ren, and J. H. Wang, Phys. Rev. B **54**, 6115 (1996).

[8] Y. Shimakawa, Y. Kubo, T. Manako, H. Igarashi, F. Izumi, and H. Asano, Phys. Rev. B **42**, 10 165 (1990).

[9] B. Morosin, D. S. Ginley, P. F. Hlava, M. J. Carr, R. J. Baughman, J. E. Schirber, E. L. Venturini, and J. F. Kwak, Physica C **152**, 413 (1988).

[10] D. E. Cox, C. C. Torardi, M. A. Subramanian, J. Gopalakrishnan, and A. W. Sleight, Phys. Rev. B **38**, 6624 (1988).

[11] M. A. Subramanian, J. B. Parise, J. C. Calabrese, C. C. Torardi, J. Gopalakrishnan, and A. W. Sleight, J. Solid State Chem. **77**, 192 (1988).

[12] N. H. Hur, B. C. Chakoumakos, M. Paranthaman, J. R. Thompson, and D. K. Christen, Physica C **253**, 109 (1995).

[13] F. Parmigiani, L. E. Depero, T. Minerva, and J. B. Torrance, J. Electron Spectrosc. Relat. Phenom. **58**, 315 (1992).

[14] G. van der Laan, C. Westra, C. Haas, and G. A. Sawatzky, Phys. Rev. B **23**, 4369 (1981).

[15] D. D. Sarma and S. G. Ovchinnikov, Phys. Rev. B **42**, 6817 (1990).

[16] J.-J. Yeh, I. Lindau, J.-Z. Sun, K. Char, N. Missert, A. Kapitulnick, T. H. Geballe, and M. R. Beasley, Phys. Rev. B **42**, 8044 (1990).

[17] F. Parmigiani and L. Sangaletti, J. Electron Spectrosc. Relat. Phenom. **66**, 223 (1994), and references therein.

[18] A. K. Santra, D. D. Sarma, and C. N. R. Rao, Phys. Rev. B **43**, 5612 (1991).

[19] C. S. Gopinath, S. Subramanian, M. Paranthaman, and A. M. Hermann, J. Solid State Chem. **109**, 211 (1994).

[20] C. N. R. Rao, G. R. Rao, M. K. Rajumon, and D. D. Sarma, Phys. Rev. B **42**, 1026 (1990).

[21] C. S. Gopinath, S. Subramanian, M. Paranthaman, and A. M. Hermann, Phys. Rev. B **48**, 15 999 (1993).

[22] T. Suzuki, M. Nagoshi, Y. Fukuda, S. Nakajima, M. Kikuchi, Y. Syono, and M. Tachiki, Physica C **162–164**, 1387 (1989).

[23] Y. Fukuda, T. Suzuki, and M. Nagoshi, in *Thallium-Based High Temperature Superconductors*, edited by A. M. Hermann and J. V. Yakhmi (Marcel Dekker, New York, 1994), Chap. 24, pp. 511–522.

[24] H. M. Meyer III, T. J. Wagener, J. H. Weaver, and D. S. Ginley, Phys. Rev. B **39**, 7343 (1989).

[25] T. Suzuki, M. Nagoshi, Y. Fukuda, Y. Syono, M. Kikuchi, N. Kobayashi, and M. Tachiki, Phys. Rev. B **40**, 5184 (1989).

[26] T. Suzuki, M. Nagoshi, Y. Fukuda, S. Nakajima, M. Kikuchi, Y. Syono, and M. Tachiki, Supercond. Sci. Technol. **7**, 817 (1994).

[27] M. P. Siegal, E. L. Venturini, B. Morosin, and T. L. Aselage, J. Mater. Res. **12**, 2825 (1997).

[28] Z. F. Ren, C. A. Wang, and J. H. Wang, Appl. Phys. Lett. **65**, 237 (1994).

[29] Z. F. Ren, C. A. Wang, J. H. Wang, D. J. Miller, D. K. Christen, J. D. Hettinger, and K. E. Gray, Physica C **258**, 129 (1995).

[30] R. P. Vasquez, M. Rupp, A. Gupta, and C. C. Tsuei, Phys. Rev. B **51**, 15 657 (1995).

[31] R. P. Vasquez and R. M. Housley, Physica C **175**, 233 (1991).

[32] R. P. Vasquez, M. C. Foote, L. Bajuk, and B. D. Hunt, J. Electron Spectrosc. Relat. Phenom. **57**, 317 (1991).

[33] R. P. Vasquez and W. L. Olson, Physica C **177**, 223 (1991).

[34] R. P. Vasquez, B. D. Hunt, M. C. Foote, L. J. Bajuk, and W. L. Olson, Physica C **190**, 249 (1992).

[35] R. P. Vasquez, J. Electron Spectrosc. Relat. Phenom. **66**, 209 (1994), and references therein.

[36] P. G. Radaelli, J. L. Wagner, B. A. Hunter, M. A. Beno, G. S. Knapp, J. D. Jorgensen, and D. G. Hinks, Physica C **216**, 29 (1993).

[37] I. M. Boswarva, Phys. Rev. B **1**, 1698 (1970).

[38] S. Larsson, Chem. Phys. Lett. **40**, 362 (1976).

[39] T. Suzuki, M. Nagoshi, Y. Fukuda, K. Oh-ishi, Y. Syono, and M. Tachiki, Phys. Rev. B **42**, 4263 (1990).

[40] P. Niedermann, A. P. Grande, J. K. Grepstad, J.-M. Triscone, M. G. Karkut, O. Brunner, L. Antognazza, W. Sadowski, H. J. Scheel, and O. Fischer, J. Appl. Phys. **68**, 1777 (1990).

[41] J. M. Tranquada, S. M. Heald, W. Kunnmann, A. R. Moodenbaugh, S. L. Qiu, Y. Xu, and P. K. Davies, Phys. Rev. B **44**, 5176 (1991).

[42] T. R. Cummins and R. G. Egdell, Phys. Rev. B **48**, 6556 (1993).

[43] J. Yu, S. Massidda, and A. J. Freeman, Physica C **152**, 273 (1988).

[44] D. R. Hamann and L. F. Mattheiss, Phys. Rev. B **38**, 5138 (1988).

[45] K. S. Kim, T. J. O'Leary, and N. Winograd, Anal. Chem. **45**, 2214 (1973).

[46] G. E. McGuire, G. K. Schweitzer, and T. A. Carlson, Inorg. Chem. **12**, 2450 (1973).

[47] B. Morosin and E. L. Venturini, Phys. Rev. B **46**, 510 (1992).

[48] R. P. Vasquez, J. Electron Spectrosc. Relat. Phenom. **66**, 241 (1994), and references therein.

[49] R. P. Vasquez, J. Electron Spectrosc. Relat. Phenom. **56**, 217 (1991).

[50] P. S. Bagus, G. Pacchioni, C. Sousa, T. Minerva, and F. Parmigiani, Chem. Phys. Lett. **196**, 641 (1992).

[51] C. Sousa, T. Minerva, G. Pacchioni, P. S. Bagus, and F. Parmi-

giani, J. Electron Spectrosc. Relat. Phenom. 63, 189 (1993).
[52] B. Morosin, R. J. Baughman, D. S. Ginley, J. E. Schirber, and E. L. Venturini, Physica C 161, 115 (1990).
[53] B. Morosin, D. S. Ginley, E. L. Venturini, R. J. Baughman, and C. P. Tigges, Physica C 172, 413 (1991).
[54] J. J. Yeh and I. Lindau, At. Data Nucl. Data Tables 32, 1 (1985).
[55] P. Marksteiner, J. Yu, S. Massidda, A. J. Freeman, J. Redinger, and P. Weinberger, Phys. Rev. B 39, 2894 (1989).